

Electrical-resistivity study on successive superconducting transitions in Ta_2S_2C

Masatsugu Suzuki* and Itsuko S. Suzuki†

Department of Physics, State University of New York at Binghamton, Binghamton, New York 13902-6000

Takashi Noji‡ and Yoji Koike§

Department of Applied Physics, Faculty of Engineering, Tohoku University, Sendai, 980-8579 JAPAN

Jürgen Walter¶

Department of Materials Science and Processing, Graduate School of Engineering,

Osaka University, 2-1, Yamada-oka, Suita, 565-0879, JAPAN

(Dated: May 24, 2019)

The superconducting properties of Ta_2S_2C have been studied from the electrical resistivity as well as the DC magnetic susceptibility. This compound undergoes successive superconducting transitions of a hierarchical nature at $T_{cl} = 3.61 \pm 0.01$ K and $T_{cu} = 9.0 \pm 0.2$ K. The resistivity ρ at $H = 0$ reduces to zero below $T_0 = 2.1$ K. The lines $T_{cu}(H)$ and $T_{cl}(H)$ merge at a point ($T_m = 2$ K and $H_m = 10$ kOe) in the H - T phase diagram. The $\ln T$ dependence of ρ at $H = 50$ kOe at low temperatures and the localized magnetic moments of conduction electrons are related to the localization effect, occurring in the 1T- TaS_2 type structure in Ta_2S_2C .

PACS numbers: 74.25.Fy, 74.25.Ha, 74.25.Dw, and 74.25.-q

I. INTRODUCTION

Ta_2S_2C has a unique layered structure, where a sandwiched structure of C-Ta-S-vdw-S-Ta-C is periodically stacked along the c axis. A van der Waals (vdw) gap is between adjacent S layers.^{1,2} The structure of Ta_2S_2C can be viewed as a structural sum of TaC and TaS_2 . The structural part corresponding to TaS_2 is identical to the atom disposition of either 1T- TaS_2 in the case of 3R- Ta_2S_2C or a hypothetical 2 H_b - TaS_2 (MoS₂-type) in the case of 1T- Ta_2S_2C (see the schematic diagram of the structure of Ta_2S_2C elsewhere^{2,3}). In our previous paper¹ we have undertaken an extensive study on the DC and AC magnetic susceptibility of Ta_2S_2C . We show that this compound undergoes successive superconducting phase transitions at T_{cl} ($= 3.61 \pm 0.01$ K) and T_{cu} ($= 9.0 \pm 0.2$ K). The intermediate phase between T_{cl} and T_{cu} is an intra-grain superconductive state, while the low temperature phase below T_{cl} is an inter-grain superconductive state.

In the present work we have measured the electrical resistivity ρ of Ta_2S_2C in the absence and the presence of an external magnetic field H . We find that the resistivity strongly depends on the temperature T and H . The resistivity ρ at $H = 0$ shows a local maximum near T_{cu} and a kink-like behavior around T_{cl} . It reduces to zero below $T_0 = 2.1$ K. Our result of ρ vs T in the presence of H is compared with the T dependence of DC and AC magnetic susceptibility.¹ The H - T phase diagram is determined based on our results of the resistivity, the DC and AC magnetic susceptibility. This phase diagram is compared with that expected for high- T_c granular superconductors.⁴

II. EXPERIMENTAL PROCEDURE

Powdered samples of Ta_2S_2C were prepared by Pablo Wally.^{5,6,7} The detail of the synthesis and structure is described in previous paper.¹ X-ray powder diffraction pattern shows that Ta_2S_2C sample consists of a 3R phase as a majority phase and a 1T phase as a minority phase. The electrical resistivity was measured using PPMS (Quantum Design) in the temperature range ($0.5 \leq T \leq 298$ K) and the magnetic field ($0 \leq H \leq 50$ kOe). The sample has a form of rectangular-prism pellet ($3.5 \times 0.8 \times 6.5$ mm³) prepared from polycrystalline powdered Ta_2S_2C by pressing it. The four-probe method was used for the measurement. The voltage probes and current probes were attached to the surface of the sample by using silver paste. The DC and AC magnetic susceptibility were measured using SQUID magnetometer (Quantum Design, MPMS XL-5). The detail of the cooling protocol process for the measurement of the zero-field cooled (ZFC) and field-cooled (FC) susceptibility is described in previous paper.¹

III. RESULT

A. Electrical resistivity

In order to study the nature of successive superconducting transitions at T_{cu} and T_{cl} in Ta_2S_2C , we have measured the electrical resistivity as a function of T and H . Figure 1 shows the T dependence of the electrical resistivity ρ at $H = 0$. In Figs. 2-4, for clarity we also show the T dependence of ρ at various magnetic field H for $0 \leq H \leq 50$ kOe, depending on the ranges of T and the values of ρ . The resistivity ρ at $H = 0$ decreases with decreasing T from 300 K, showing a metallic be-

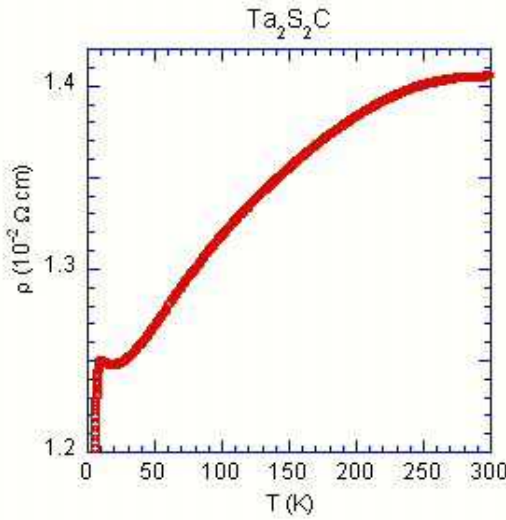


FIG. 1: (Color online) T dependence of the resistivity ρ at $H = 0$ for $\text{Ta}_2\text{S}_2\text{C}$.

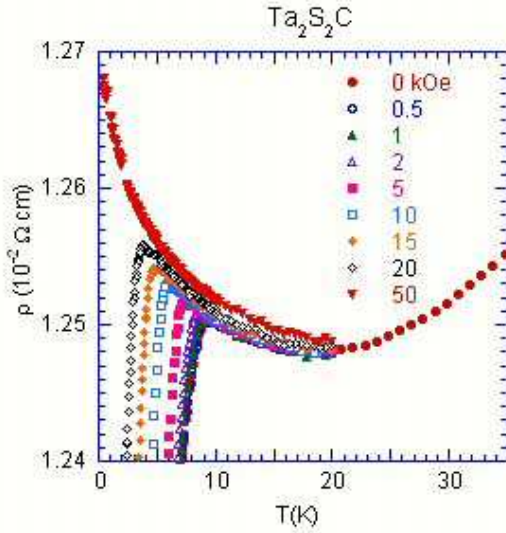


FIG. 2: (Color online) T dependence of ρ at fixed H ($= 0, 0.5, 1, 2, 5, 10, 15, 20$, and 50 kOe).

havior at high temperatures: As shown in Fig. 2, ρ at $H = 0$ shows a local minimum at T_{min} ($= 19$ K), and starts to increase with decreasing T , showing a bit of evidence for the possible localization effect mainly occurring in the TaS_2 layer of the system. The resistivity ρ at $H = 0$ exhibits a local maximum at T_{max} (≈ 9.6 K) and again starts to decreases with decreasing T . This local-maximum temperature T_{max} coincides with the upper critical temperature T_{cu} determined from our DC and AC magnetic susceptibility measurements. As shown in Fig. 3 and Fig. 4 (a), ρ at $H = 0$ exhibits a kink-like behavior at T_{kink} (≈ 3.6 K). This kink temperature corresponds to the lower critical temperature T_{cl} determined from our DC and AC magnetic susceptibility.¹ The re-

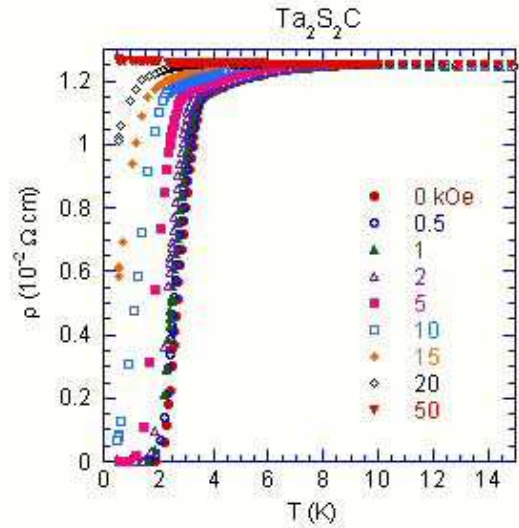


FIG. 3: (Color online) T dependence of ρ at various H below 15 K.

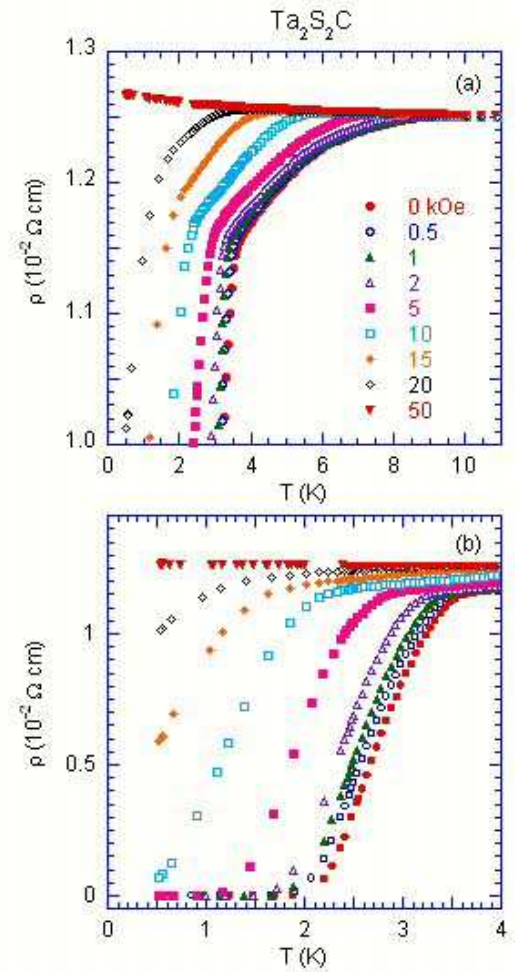


FIG. 4: (Color online) (a) and (b) T dependence of ρ at low temperatures for various H .

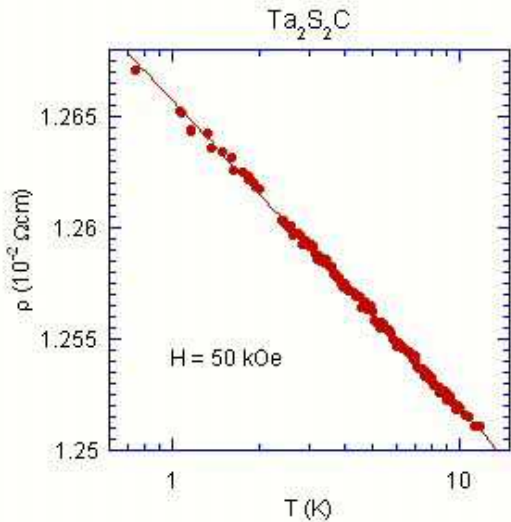


FIG. 5: (Color online) T dependence of resistivity at $H = 50$ kOe for $0.7 \leq T \leq 12$ K. The solid line denotes the least-squares fitting curve to Eq.(1)

sistivity ρ drastically decreases with decreasing T below T_{kink} and reduces to zero below $T_0 = 2.1$ K, suggesting that the superconductivity occurs at low T over the whole system. For convenience, we also define the characteristic temperature $T_{1/2}$ at which ρ is equal to a half of the normal resistivity at T_{max} . As shown in Figs. 2-4, the curve of ρ vs T is strongly dependent on H . The characteristic temperatures T_{max} , T_{kink} , $T_{1/2}$ and T_0 decrease with increasing H . The H - T diagram of these temperatures will be described in Sec. III C and is compared with that of T_{cu} and T_{cl} .¹

It seems that the local minimum temperature $T_{min}(H)$ for ρ vs T is independent of H for $0 \leq H \leq 50$ kOe (see Fig. 2). The curve of $\rho(H, T)$ vs T for $0 \leq H \leq 20$ kOe deviates from that at $H = 50$ kOe at low temperatures below $T_{max}(H)$. No local maximum in ρ vs T is observed at $H = 50$ kOe: ρ continues to increase with decreasing T at least down to $T = 0.5$ K. Figure 5 shows the plot of ρ at $H = 50$ kOe as a function of a logarithmic scale of T for $0.7 \leq T \leq 12$ K. We find that ρ is well described by

$$\rho = \rho_0 - \rho_1 \ln T \quad (1)$$

with $\rho_0 = 12.66$ mΩcm and $\rho_1 = 5.99 \times 10^{-2}$ mΩcm. This suggests that the mutual interaction effect between electrons in a 2D weakly localized state⁸ occurs in the system at $H = 50$ kOe. In our previous paper, we show that the susceptibility χ_{FC} at $H = 10$ kOe consists of a Curie-type behavior at low T due to the localized electron spins related to the Anderson localization. The superconducting state competes with the localization state, depending on the strength of H . The superconducting state is energetically favorable for $H = 20$ kOe, while the superconducting state is suppressed and the localization state becomes favorable at $H = 50$ kOe. The supercon-

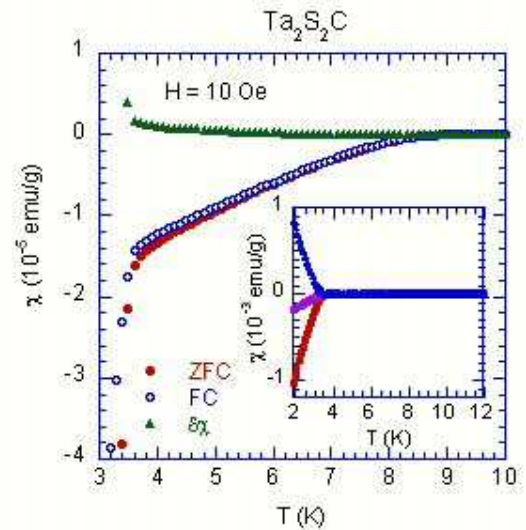


FIG. 6: (Color online) T dependence of the zero-field cooled susceptibility χ_{ZFC} , the field-cooled susceptibility χ_{FC} , and the difference $\delta\chi$ ($= \chi_{FC} - \chi_{ZFC}$) for $H = 10$ Oe.

ducting state mainly occurs in the TaC layers, while the localized state occurs in the TaS₂ layer.¹

It is interesting to compare our results of ρ vs T at $H = 50$ kOe with that at $H = 0$ for 1T-TaS₂.⁹ The overall behavior of ρ vs T at $H = 50$ kOe is qualitatively similar to that of 1T-TaS₂ at least below the charge density wave (CDW) commensurate transition temperature T_d (≈ 200 K).⁹ The resistivity ρ at $H = 0$ for 1T-TaS₂ shows a local minimum around 50 K and increases with further decreasing T . The value of ρ , which is between 30 and 40 mΩcm, is relatively larger than that (≈ 12.5 mΩcm) for ρ at $H = 50$ Oe for Ta₂S₂C (see Fig. 2).

We note that for 1T-TaS₂, the resistivity ρ below 2 K diverges according to the relation $\rho = \rho_a \exp[(T_a/T)^n]$ with $n = 1/3$, where ρ_a is a constant resistivity and T_a is a characteristic temperature.⁹ This is characteristic of the 2D variable-range hopping conduction in a strongly Anderson-localized state due to a random potential.

Our result of ρ vs T is rather different from that of Ta₂S₂C reported by Ziebarath et al.¹⁰ using a pressed-and sintered sample. They have observed that ρ increases with increasing T for $4.2 \leq T \leq 300$ K ($\rho \approx 0.8$ mΩcm at 4.2 K and 2.2 mΩcm at 300 K), showing a metallic behavior. No discontinuous change in ρ has been seen below 300 K.

B. χ_{ZFC} and χ_{FC}

Our results on the zero-field cooled susceptibility χ_{ZFC} and the field-cooled susceptibility χ_{FC} have been reported in detail in our previous paper.¹ These results are consistent with the present results derived from the measurement of ρ vs T (Sec. III A). Here we summarize our results using two figures which are not published in

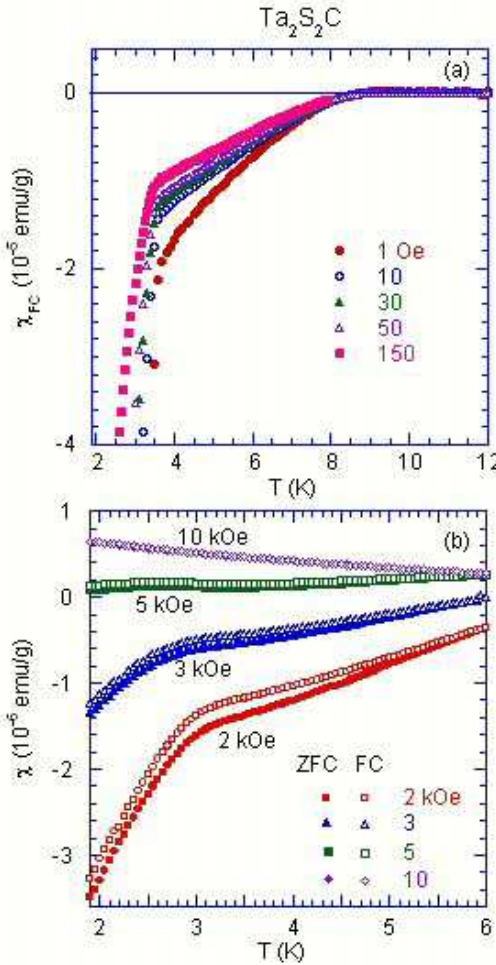


FIG. 7: (Color online) a) T dependence of χ_{FC} at $H = 1, 10, 30, 50$, and 150 Oe. (b) T dependence of χ_{FC} and χ_{ZFC} at $H = 2, 3, 5$, and 10 kOe.

the previous paper.¹ The method of the measurements is the same as that in the previous paper.¹ Figure 6 shows the T dependence of χ_{ZFC} , χ_{FC} , and the difference $\delta\chi$ at $H = 10$ Oe, where $\delta\chi = \chi_{\text{FC}} - \chi_{\text{ZFC}}$. Figure 7(a) shows the T dependence of χ_{FC} for $1 \leq H \leq 150$ Oe. Figure 7(b) shows the T dependence of χ_{ZFC} and χ_{FC} for $H \geq 2$ kOe. In Fig. 6 and Fig. 7(a), the susceptibility χ_{ZFC} (χ_{FC}) exhibits a kink at $T_{\text{cl}}(H)$, where $d\chi_{\text{ZFC}}/dT$ ($d\chi_{\text{FC}}/dT$) undergoes a discontinuous jump. The deviation of χ_{ZFC} from χ_{FC} is clearly seen below $T_{\text{cl}}(H)$, indicating that the extra magnetic flux is trapped during the FC process (see more detail of $\delta\chi$ vs T at various H in our previous paper¹). Between $T_{\text{cl}}(H)$ and $T_{\text{cu}}(H)$, $\delta\chi$ is still positive but nearly equal to zero.

As shown in Fig. 7(b), there is a drastic decrease in the diamagnetic contribution in χ_{ZFC} with increasing T below $T_{\text{cl}}(H)$. Nevertheless, a diamagnetic contribution in χ_{ZFC} still remains above $T_{\text{cl}}(H)$, increases with fur-

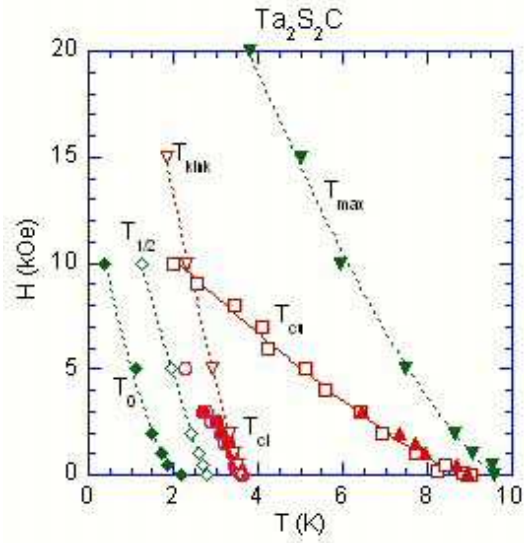


FIG. 8: (Color online) H - T phase diagram. The characteristic temperatures (T_0 , $T_{1/2}$, T_{kink} , T_{max}) are defined from the resistivity measurement; T_0 where ρ reduces to zero, $T_{1/2}$ where ρ is equal to one half of the normal resistivity, T_{kink} where ρ shows a kink-like behavior, and T_{max} where ρ exhibits a local maximum. The critical temperatures (T_{cu} and T_{cl}) are defined from the DC and AC magnetic susceptibility,¹ T_{cl} is determined from the measurements of χ' ($f = 1$ Hz) vs T and χ'' ($f = 1$ Hz) vs T . T_{cu} is determined from the measurements of χ' ($f = 1$ Hz) vs T and χ_{ZFC} vs T . The solid line is least-squares fitting curve for the data of $T_{\text{cu}}(H)$ to Eq.(2). The dotted lines are guide to the eyes.

ther increasing T , and becomes zero at a upper critical temperature $T_{\text{cu}}(H)$. The sign of χ_{ZFC} changes from negative to positive around 9 K with increasing T .¹ At $H = 5$ kOe, χ_{ZFC} is positive at least between 1.9 and 6 K, showing a broad peak at 2.65 K. At $H = 10$ kOe, χ_{ZFC} decreases with increasing T , showing a Curie-like behavior.¹ We note that the susceptibility at low T for 1T-TaS₂ shows a Curie-like behavior due to the localized magnetic moments of conduction electrons related to the Anderson localization effect.⁹

C. H - T phase diagram

Figure 8 shows the H - T phase diagram. Here $T_{\text{cl}}(H)$ is determined from the data of χ' vs T and χ'' vs T , and $T_{\text{cu}}(H)$ is determined from the data of χ_{ZFC} vs T (see the previous paper¹ in detail). The negative sign of χ_{ZFC} and χ' below $T_{\text{cu}}(H)$ indicates that the system is at least partially in a superconducting state. The dispersion χ' shows a kink-like behavior at $T_{\text{cl}}(H)$. Four characteristic temperatures are determined from the resistivity measurement: (i) T_0 where ρ reduces to zero, (ii) $T_{1/2}$ where ρ is equal to one half of the normal resistivity, (iii) T_{kink} where ρ shows a kink-like behavior, and (iv) T_{max} where ρ exhibits a local maximum. As shown in

Fig. 8, the line $T_{kink}(H)$ almost coincides with the line $T_{cl}(H)$. The line $T_{max}(H)$ is near the line $T_{cu}(H)$ at low H but the difference between them becomes larger as H increases. This may be due to the superconducting fluctuations sensitively observed by the resistivity measurements. The lines $T_0(H)$ and $T_{1/2}(H)$ are a little lower than the line $T_{cl}(H)$ at the same H by 1.2 - 1.5 K. This difference may be reduced when the structural coupling between fine particles in the pelletized sample becomes strong during the pressing process. It seems that the lines $T_{cu}(H)$ and $T_{kink}(H)$ merge into a point located at $H_m = 10$ kOe and $T_m = 2$ K in the H - T plane. In the previous paper¹ we assume that the line $T_{cu}(H)$ corresponds to the upper critical fields $H_{c2}^{(u)}(T)$. The line $H_{c2}^{(u)}(T)$ can be well described by

$$H_{c2}^{(u)}(T) = H_{c2}^{(u)}(T=0)(1 - \frac{T}{T_{cu}})^\alpha, \quad (2)$$

with $\alpha = 1.23 \pm 0.07$, $T_{cu} = 8.9 \pm 0.1$ K, and $H_{c2}^{(u)}(T=0) = 14.5 \pm 0.5$ kOe.¹

IV. DISCUSSION

In the previous paper,¹ we have estimated the coherence length (ξ) and the penetration depth (λ) as $\xi = 210 \pm 10 \text{ \AA}$ and $\lambda = 4200 \pm 100 \text{ \AA}$, respectively. As long as the coherence length ξ is larger than the grain size d , the detailed structure of the disordered system is not so important and the system behaves like an ordinary homogeneous superconductor. In this case we can assume that the system is formed of a type II superconductor surrounded by a matrix of Josephson junctions. Our result of Fig. 8 is qualitatively in good agreement with the H - T phase diagram of granular superconductors predicted by Gerber et al.⁴ in the limiting case when the lower critical field is almost equal to zero. The line $T_{cu}(H)$ intersects with the line $T_{cl}(H)$ at $T = T_m = 2$ K and $H = H_m = 10$ kOe. The resistivity becomes zero on the line $T_0(H)$, indicating the long range superconducting order becomes established over the whole system. Note that the line $T_0(H)$ may coincide with the line $T_{cl}(H)$ for the system where the structural coupling between fine particles is strong compared to that in the present system.

The possible existence of mesoscopic grains in the TaC-type layers of $\text{Ta}_2\text{S}_2\text{C}$ would be essential to the successive transitions having a hierarchical nature. In the intermediate phase between T_{cu} and T_{cl} , each grain in TaC layers becomes a superconductor. Through the intra-planar Josephson coupling between grains, the region of

the superconducting grains becomes larger as T decreases below T_{cu} , forming a 2D superconducting phase. Below T_{cl} , the effective interplanar Josephson coupling becomes strong enough to give rise to a 3D superconducting phase.

Similar behaviors in the T dependence of ρ at $H = 0$, and χ_{ZFC} and χ_{FC} at $H = 0.1$ Oe has been reported for the high-temperature superconductor ceramics $\text{YB}_2\text{Cu}_4\text{O}_8$. Successive superconducting transitions occur at T_{cu} and T_{cl} .^{11,12,13} A negative nonlinear magnetic susceptibility and a negative nonlinear electrical resistivity are observed at T_{cl} in the absence of H . These behaviors can be explained in terms of a 3D XY chiral glass model,¹⁴ where the frustration effect arises from the random distribution of π junctions with the negative Josephson coupling. In spite of the similarity between our result and the results on $\text{YB}_2\text{Cu}_4\text{O}_8$, it seems that our result is not directly related to the 3D XY chiral glass model, because of no anisotropic pairing symmetry of the $d_{x^2-y^2}$ wave type in our system. So far no experiment concerning the nonlinear magnetic susceptibility and nonlinear electrical resistivity around T_{cl} has been made. The mechanism for the superconducting transition at T_{cl} is not yet well understood at the present stage.

V. CONCLUSION

$\text{Ta}_2\text{S}_2\text{C}$ undergoes successive superconducting transitions of a hierarchical nature at $T_{cl} = 3.61 \pm 0.01$ K and $T_{cu} = 9.0 \pm 0.2$ K. The intermediate phase between T_{cu} and T_{cl} is an intra-grain superconductive state occurring in the TaC-type structure in $\text{Ta}_2\text{S}_2\text{C}$, while the low temperature phase below T_{cl} is an inter-grain superconductive state. The resistivity ρ shows a local maximum around $T_{cu}(H)$ and a kink-like behavior at $T_{kink}(H)$ ($\approx T_{cl}(H)$). The $\ln T$ dependence of ρ at $H = 50$ kOe at low temperatures is due to the 2D weak localization effect occurring in the 1T-TaS₂-type structure in $\text{Ta}_2\text{S}_2\text{C}$.

Acknowledgments

The authors are grateful to Pablo Wally, Technical University of Vienna, Austria (now Littlefuse, Yokohama, Japan) for providing them with the samples. The work at the Tohoku University was partly supported by a Grant-in-Aid for Scientific Research from the Ministry of Education, Culture, Sports, Science and Technology, Japan.

* suzuki@binghamton.edu

† itsuko@binghamton.edu

‡ noji@teion.apph.tohoku.ac.jp

§ koike@teion.apph.tohoku.ac.jp

¶ Juerg.Walter@t-online.de

¹ J. Walter, I.S. Suzuki, and M. Suzuki, Phys. Rev. B **70**,

- 064519 (2004), and see References therein.
- ² O. Beckmann, H. Boller, H. Nowotny, *Monatsch. Chem.* **101**, 945 (1970).
- ³ K. Sakamaki, H. Wada, H. Nozaki, Y. Ōnuki, and M. Kawai, *J. Alloys and Compounds* **339**, 283 (2002).
- ⁴ A. Gerber, Th. Grenet, M. Cyrot, and J. Beille, *Phys. Rev. B* **45**, 5099 (1992).
- ⁵ P. Wally and M. Ueki, *J. Solid State Chem.* **138**, 250 (1998).
- ⁶ P. Wally and M. Ueki, *J. Alloys and Compounds* **268**, 83 (1998).
- ⁷ P. Wally and M. Ueki, *Wear* **215**, 98 (1998).
- ⁸ H. Fukuyama, *Physica B+C* **117** & **118**, 676 (1983).
- ⁹ F.J. DiSalvo and J.V. Waszczak, *Phys. Rev. B* **22**, 4241 (1980).
- ¹⁰ R.P. Ziebarth, J.K. Vassiliou, and F.J. Di Salvo, *J. Less-Common Metals* **156**, 207 (1989).
- ¹¹ M. Kawachi, M. Hagiwara, K. Koyama, and M. Matsuura, *J. Phys. Soc. Jpn.* **63**, 3405 (1994).
- ¹² M. Matsuura, M. Kawachi, K. Miyoshi, M. Hagiwara, and K. Koyama, *J. Phys. Soc. Jpn.* **64**, 4540 (1995).
- ¹³ T. Yamao, M. Hagiwara, K. Koyama, and M. Matsuura, *J. Phys. Soc. Jpn.* **68**, 971 (1999).
- ¹⁴ H. Kawamura and M.S. Li, *J. Phys. Soc. Jpn.* **66**, 2110 (1997).